

FDR-Corrected Sparse Canonical Correlation Analysis with Applications to Imaging Genomics

Alexej Gossmann, Pascal Zille, Vince Calhoun, and Yu-Ping Wang

Abstract—Reducing the number of false positive discoveries is presently one of the most pressing issues in the life sciences. It is of especially great importance for many applications in neuroimaging and genomics, where datasets are typically high-dimensional, which means that the number of explanatory variables exceeds the sample size. The false discovery rate (FDR) is a criterion that can be employed to address that issue. Thus it has gained great popularity as a tool for testing multiple hypotheses. Canonical correlation analysis (CCA) is a statistical technique that is used to make sense of the cross-correlation of two sets of measurements collected on the same set of samples (e.g., brain imaging and genomic data for the same mental illness patients), and sparse CCA extends the classical method to high-dimensional settings. Here we propose a way of applying the FDR concept to sparse CCA, and a method to control the FDR. The proposed FDR correction directly influences the sparsity of the solution, adapting it to the unknown true sparsity level. Theoretical derivation as well as simulation studies show that our procedure indeed keeps the FDR of the canonical vectors below a user-specified target level. We apply the proposed method to an imaging genomics dataset from the Philadelphia Neurodevelopmental Cohort. Our results link the brain activity during a working memory task, as measured by functional magnetic resonance imaging (fMRI), to the corresponding subjects' genomic data. Our findings are supported by previous work on cognitive ability, neurodevelopmental, and other mental disorders.

Index Terms—fMRI analysis, Genome, Machine learning, Probabilistic and statistical methods.

I. INTRODUCTION

CANONICAL correlation analysis (due to Hotelling, [1]), or CCA, is a classical statistical technique, which is used to make sense of the cross-correlation of two sets of measurements collected on the same set of samples. More precisely, given two sets of random variables, CCA identifies linear combinations of each, which have maximum correlation with each other. The coefficients of these linear combinations of features are called canonical vectors. Like many classical statistical techniques, CCA fails in high-dimensional settings, when the number of variables in either of the two cross-correlated datasets exceeds the number of samples. For application to high-dimensional data, several methods of sparse canonical correlation analysis (sparse CCA, or sCCA) have been proposed, where sparsity is imposed on the canonical

vectors (e.g., see [2]–[4]). Many applications have demonstrated the usefulness of sparse CCA methods. For example they are commonly used in genomics to analyze datasets consisting of two genomic assays for the same set of subjects or cells (e.g., [5], [6] among many others). They have also been successfully employed for the analysis of neuroimaging and imaging genomics datasets (e.g., [7], [8]), such as brain imaging and DNA sequence data for the same set of brain disease or mental illness patients.

However, most of the widely used sparse CCA methods determine the level of sparsity of the canonical vectors based on criteria of model fit. Different types of cross-validation procedures have been proposed for sparse CCA (e.g., [4], [6], [8]), sometimes incorporating criteria such as the AIC or BIC (e.g., [9]), and a permutation based method is proposed in [3]. In some cases authors simply impose a certain level of sparsity on the solution vectors (e.g., [5]), which heavily relies on the appropriateness of such prior assumptions. In general, the behaviour of the selection procedures for the sparsity parameters in sparse CCA is not well understood, and there is a lack of theoretical guarantees regarding the recovery of an appropriate sparsity level of the sparse CCA solution.

In this work we propose a definition of false discovery rate (FDR) for canonical vectors, which is subsequently used as a statistical criterion to determine an appropriate sparsity level for a sparse CCA solution. The proposed FDR criterion is a generalization of the conventional FDR [10] to canonical correlation analysis. With the aim of reliably obtaining canonical vectors with FDR below a user-specified level q , we propose an *FDR-corrected sparse CCA* procedure. Up to a (small) proportion of false discoveries, which our method keeps on average far below a user-specified level q , the FDR-corrected sparse CCA method is shown to produce canonical vectors consisting only of features that are truly cross-correlated between the two analyzed datasets. Roughly, our proposed procedure consists of the following two steps: (1) we use a subsample of the data to fit a (conventional) sparse CCA model; and (2) we use the remainder of the dataset to perform an FDR correction on the result of step (1).

With a theoretical derivation as well as simulation studies we show that our procedure indeed keeps the FDR of the canonical vectors below a user-specified target level. Additionally, we apply our method to an imaging genomics dataset from the Philadelphia Neurodevelopmental Cohort. We analyze subjects' brain activity during a working memory task, as measured by functional magnetic resonance imaging (fMRI), in conjunction with the subjects' DNA sequence data. The goal is to gain understanding in how genetic variation

A. Gossmann is with the Bioinnovation PhD Program, Tulane University, New Orleans, LA. Web: <http://www.alexejgossmann.com>.

Y.-P. Wang and P. Zille are with the Department of Biomedical Engineering, Tulane University, New Orleans, LA.

V. Calhoun is with The Mind Research Network, and the Department of Electrical and Computer Engineering, University of New Mexico, Albuquerque, NM.

influences the brain activity fMRI data during a working memory task. Our real data results are consistent with those reported elsewhere in the literature, demonstrating the validity of the method.

II. CANONICAL CORRELATION ANALYSIS

In this section we describe the data structure and the notation that we use throughout the rest of the paper. This section also introduces the classical CCA method, as well as the standard approach to sparse CCA.

A. Assumed data structure and notation

Let $\mathbf{x}^{(1)}, \mathbf{x}^{(2)}, \dots, \mathbf{x}^{(n)} \in \mathbb{R}^{p_X}$ be independent $\mathcal{N}(0, \Sigma_X)$ -distributed vectors, and let $\mathbf{y}^{(1)}, \mathbf{y}^{(2)}, \dots, \mathbf{y}^{(n)} \in \mathbb{R}^{p_Y}$ be independent $\mathcal{N}(0, \Sigma_Y)$ -distributed vectors, where $\Sigma_X \in \mathbb{R}^{p_X \times p_X}$ and $\Sigma_Y \in \mathbb{R}^{p_Y \times p_Y}$ are symmetric positive definite.

Assume that for all $k \in \{1, \dots, n\}$, the cross-covariance matrix

$$\text{Cov}(\mathbf{x}^{(k)}, \mathbf{y}^{(k)}) = \Sigma_{XY} \in \mathbb{R}^{p_X \times p_Y}$$

has entries $\rho_{i,j}^{XY}$ for $i \in \{1, \dots, p_X\}$ and $j \in \{1, \dots, p_Y\}$, and assume that

$$\text{Cov}(\mathbf{x}^{(k)}, \mathbf{y}^{(l)}) = 0, \text{ if } k \neq l.$$

Similarly, for $i, j \in \{1, \dots, p_X\}$ we denote the entries of Σ_X by $\rho_{i,j}^X$, and the entries of Σ_Y by $\rho_{i,j}^Y$ for $i, j \in \{1, \dots, p_Y\}$.

We define random matrices $X \in \mathbb{R}^{n \times p_X}$ and $Y \in \mathbb{R}^{n \times p_Y}$ by

$$X := \begin{bmatrix} (\mathbf{x}^{(1)})^T \\ (\mathbf{x}^{(2)})^T \\ \vdots \\ (\mathbf{x}^{(n)})^T \end{bmatrix}, \quad Y := \begin{bmatrix} (\mathbf{y}^{(1)})^T \\ (\mathbf{y}^{(2)})^T \\ \vdots \\ (\mathbf{y}^{(n)})^T \end{bmatrix}.$$

Thus, we can think of X and Y as two datasets containing respectively p_X and p_Y features collected for n independent samples, where the features in the two datasets are cross-correlated with cross-covariance matrix Σ_{XY} . In that sense, the matrix $\begin{bmatrix} X & Y \end{bmatrix}$ is the combined dataset with covariance structure given by the matrix

$$\Sigma := \begin{bmatrix} \Sigma_X & \Sigma_{XY} \\ \Sigma_{XY}^T & \Sigma_Y \end{bmatrix}. \quad (1)$$

Please note that even though all presented analytical derivations pre-suppose Gaussian data, we investigate departures from this distributional assumption in the simulation studies of Section V-B.

B. Classical CCA

Standard formulation of CCA [1] seeks for vectors $\mathbf{u} \in \mathbb{R}^{p_X}$ and $\mathbf{v} \in \mathbb{R}^{p_Y}$ to maximize the sample correlation between $X\mathbf{u}$ and $Y\mathbf{v}$. Thus, the CCA optimization problem is given by

$$\arg \max_{\mathbf{u} \in \mathbb{R}^{p_X}, \mathbf{v} \in \mathbb{R}^{p_Y}} \widehat{\text{Cov}}(X\mathbf{u}, Y\mathbf{v}) = \arg \max_{\mathbf{u} \in \mathbb{R}^{p_X}, \mathbf{v} \in \mathbb{R}^{p_Y}} \frac{1}{n} \mathbf{u}^T X^T Y \mathbf{v},$$

subject to

$$\begin{aligned} \widehat{\text{Var}}(X\mathbf{u}) &= \frac{1}{n-1} \mathbf{u}^T X^T X \mathbf{u} = 1, \\ \widehat{\text{Var}}(Y\mathbf{v}) &= 1. \end{aligned}$$

The solution to this optimization problem, $(\widehat{\mathbf{u}}, \widehat{\mathbf{v}})$, is called the first pair of canonical vectors. The linear combinations of features, $X\widehat{\mathbf{u}}$ and $Y\widehat{\mathbf{v}}$, are called the first pair of canonical variates. Subsequent pairs of canonical variates are restricted to be uncorrelated with the previous ones. For more detail we refer to [11].

C. Sparse CCA

The conventional CCA becomes degenerate if $n \leq \max\{p_X, p_Y\}$, which is often the case in neuroimaging and other biomedical applications. Sparse CCA (e.g., [2]–[4]) extends CCA to high-dimensional data by imposing a sparsity assumption on the CCA solution. Sparsity is achieved by utilizing penalty terms, such as the ℓ_1 -norm, on the canonical vectors. This results in a unique solution even when $p_X, p_Y \gg n$.

Most commonly the ℓ_1 -penalty is used in order to enforce the sparsity assumption on the canonical vectors. The resulting penalized CCA problem, which is introduced in [2], is given by

$$\arg \max_{\mathbf{u} \in \mathbb{R}^{p_X}, \mathbf{v} \in \mathbb{R}^{p_Y}} \frac{1}{n} \mathbf{u}^T X^T Y \mathbf{v},$$

subject to

$$\|\mathbf{u}\|_2^2 \leq 1, \|\mathbf{v}\|_2^2 \leq 1, \|\mathbf{u}\|_1 \leq c_1, \|\mathbf{v}\|_1 \leq c_2.$$

However, the determination of the sparsity level, or the model tuning parameters c_1 and c_2 , remains a challenging problem, and a topic of ongoing research, as briefly discussed in Section I.

Higher-order pairs of canonical vectors can be found by applying sparse CCA to a residual matrix, obtained from $X^T Y$ and the previously found canonical variates (see [2]).

III. DEFINING FALSE DISCOVERY RATE (FDR) FOR SPARSE CCA

It is not clear how the well-known definition of FDR (due to [10]), which is widely used in multiple hypothesis testing, can be carried over to sparse CCA. In this work, we first propose an adaptation of the FDR concept to the context of sparse CCA, and then introduce a method which ensures that the FDR is kept below a given threshold. Since we have a pair of canonical vectors \mathbf{u} and \mathbf{v} , we consider the FDR in \mathbf{u} and in \mathbf{v} separately. For the sake of clarity, we present in the following the FDR derivation for the canonical vector \mathbf{u} only. An identical derivation can be used for the canonical vector \mathbf{v} .

The problem of identifying, which entries of \mathbf{u} are truly non-zero, can be recast as p_X hypotheses tests

$$H_i : u_i = 0, \quad i \in \{1, 2, \dots, p_X\}, \quad (2)$$

where we consider the null hypothesis H_i to be true if

$$(\forall j \in \{1, 2, \dots, p_Y\}) : \rho_{i,j}^{XY} = 0,$$

that is, if the i th feature in X is uncorrelated with all features in Y .

Let $R_{\hat{\mathbf{u}}}$ be the number of non-zero entries in the sparse CCA estimate $\hat{\mathbf{u}}$, that is, the number of the rejected H_i . Let $V_{\hat{\mathbf{u}}}$ denote the number of false rejections, that is, the number of indices $i \in \{1, 2, \dots, p_X\}$, such that $\hat{u}_i \neq 0$ but $\rho_{i,j}^{XY} = 0$ for all $j \in \{1, 2, \dots, p_Y\}$.

Analogously, define $R_{\hat{\mathbf{v}}}$ and $V_{\hat{\mathbf{v}}}$ for the canonical vector $\hat{\mathbf{v}}$.

Definition 1 (False discovery rate). Define the false discovery rate in \mathbf{u} as

$$\text{FDR}(\hat{\mathbf{u}}) := \mathbb{E} \left(\frac{V_{\hat{\mathbf{u}}}}{\max\{R_{\hat{\mathbf{u}}}, 1\}} \right), \quad (3)$$

and analogously define,

$$\text{FDR}(\hat{\mathbf{v}}) := \mathbb{E} \left(\frac{V_{\hat{\mathbf{v}}}}{\max\{R_{\hat{\mathbf{v}}}, 1\}} \right). \quad (4)$$

In the next section we rely on this definition of FDR as an optimality criterion and as a guide in the identification of an appropriate sparsity level for the canonical vectors.

IV. FDR-CORRECTED SPARSE CCA

Solving the classical CCA problem of Section II-B via the singular value decomposition (SVD), we see that the canonical vector \mathbf{u} is given (up to a scaling constant) by $X^T Y \mathbf{v}$. Likewise, the canonical vector \mathbf{v} can be written up to scaling as $Y^T X \mathbf{u}$. That is, using the symbol “ \propto ” for “proportional to”, we have that

$$\mathbf{u} \propto X^T Y \mathbf{v}, \quad (5)$$

$$\mathbf{v} \propto Y^T X \mathbf{u}, \quad (6)$$

Thus, for purposes of controlling FDR in \mathbf{u} , the hypotheses tests given by Equation (2) are equivalent to testing

$$H_i : (X^T Y \mathbf{v})_i = 0, \quad i \in \{1, 2, \dots, p_X\},$$

and analogously for \mathbf{v} .

Motivated by that observation, the main idea of our FDR-correcting approach is to first obtain initial estimates $\hat{\mathbf{u}}^{(0)}$ and $\hat{\mathbf{v}}^{(0)}$ of the canonical vectors, and then to test null hypotheses of the form

$$H_i^{(u)} : (X^T Y \hat{\mathbf{v}}^{(0)})_i = 0, \quad i = 1, 2, \dots, p_X, \quad (7)$$

and

$$H_j^{(v)} : (Y^T X \hat{\mathbf{u}}^{(0)})_j = 0 \quad j = 1, 2, \dots, p_Y, \quad (8)$$

in order to determine which entries of \mathbf{u} and \mathbf{v} are truly non-zero.

A. Asymptotic distribution

In order to be able to make probabilistic statements about the estimators of the sparse canonical vectors, we need to know the respective distributions of $X^T Y \mathbf{v}$ and $Y^T X \mathbf{u}$. In the following we will focus on $X^T Y \mathbf{v}$, but the obtained results clearly carry over to $Y^T X \mathbf{u}$, by swapping X and Y as well as \mathbf{u} and \mathbf{v} .

Theorem 1 (Asymptotic Normality). *Let the random matrices X and Y be defined as above. For any vector $\mathbf{v} \in \mathbb{R}^{p_Y}$, it holds that*

$$\sqrt{n} \left(\frac{1}{n} X^T Y \mathbf{v} - \boldsymbol{\mu} \right) \xrightarrow{\mathcal{D}} \mathcal{N}(0, \Omega), \quad (9)$$

where $\boldsymbol{\mu} \in \mathbb{R}^{p_X}$ has entries

$$\mu_i = \sum_{j=1}^{p_Y} v_j \rho_{i,j}^{X,Y}, \quad (10)$$

and where $\Omega \in \mathbb{R}^{p_X \times p_X}$ has entries

$$\omega_{i,j} = \left(\sum_{k=1}^{p_Y} v_k \rho_{i,k}^{X,Y} \right) \left(\sum_{k=1}^{p_Y} v_k \rho_{j,k}^{X,Y} \right) + \rho_{i,j}^{X,Y} \mathbf{v}^T \Sigma_Y \mathbf{v}. \quad (11)$$

Proof. The proof is given in Appendix A. \square

B. The FDR-corrected sparse CCA procedure

We propose an FDR correction procedure for sparse CCA consisting of the following steps:

1. *Subset the data.* We divide each of the data matrices X and Y into two subsets of sizes n_0 and n_1 (with $n_0 + n_1 = n$).

$$X = \begin{bmatrix} X^{(0)} \\ X^{(1)} \end{bmatrix}, \quad \text{where } X^{(0)} \in \mathbb{R}^{n_0 \times p_X}, X^{(1)} \in \mathbb{R}^{n_1 \times p_X},$$

$$Y = \begin{bmatrix} Y^{(0)} \\ Y^{(1)} \end{bmatrix}, \quad \text{where } Y^{(0)} \in \mathbb{R}^{n_0 \times p_Y}, Y^{(1)} \in \mathbb{R}^{n_1 \times p_Y}.$$

2. *Obtain preliminary parameter estimates on the first set.* We apply a sparse CCA algorithm of our choice to $X^{(0)}$ and $Y^{(0)}$, in order to obtain estimated sparse canonical vectors $\hat{\mathbf{u}}^{(0)}$ and $\hat{\mathbf{v}}^{(0)}$. In this paper we use the popular ℓ_1 -penalized CCA [2] with a liberal choice for the tuning parameters¹, with the goal of capturing all truly non-zero entries of the true canonical vectors \mathbf{u} and \mathbf{v} within the support of the estimates $\hat{\mathbf{u}}^{(0)}$ and $\hat{\mathbf{v}}^{(0)}$. Furthermore, we use $X^{(0)}$ and $Y^{(0)}$ to obtain $\hat{\Sigma}^{(0)}$, the maximum likelihood estimate of the covariance matrix of $\begin{bmatrix} X & Y \end{bmatrix}$.
3. *Obtain p -values using the second set.* Now, Theorem 1 implies the approximation

$$\left(\frac{1}{\sqrt{n}} \left(X^{(1)} \right)^T Y^{(1)} \hat{\mathbf{v}}^{(0)} \middle| \Sigma = \hat{\Sigma}^{(0)} \right) \sim \mathcal{N} \left(\sqrt{n} \hat{\boldsymbol{\mu}}^{(0)}, \hat{\Omega}^{(0)} \right),$$

where $\hat{\boldsymbol{\mu}}^{(0)}$ and $\hat{\Omega}^{(0)}$ are defined according to equations (10) and (11) with $\hat{\mathbf{v}}^{(0)}$ and $\hat{\Sigma}^{(0)}$ substituted

¹The exact strategy of choosing the penalty parameters in this step is presented for each considered application of the procedure, at the time when the respective application is discussed in Sections V-A, V-B, and VI.

in place of \mathbf{v} and Σ (recall that Σ_X , Σ_Y , and Σ_{XY} denote the corresponding blocks of Σ , which have entries $\rho_{i,j}^X$, $\rho_{i,j}^Y$, and $\rho_{i,j}^{XY}$). Analogously, from Theorem 1 we obtain an asymptotic distribution for $\left(\frac{1}{\sqrt{n}}(Y^{(1)})^T X^{(1)}\hat{\mathbf{u}}^{(0)}\right) \Big| \Sigma = \hat{\Sigma}^{(0)}$.

We obtain p-values for the hypotheses tests (7) and (8) based on these asymptotic distributions.

4. *Apply an FDR correcting procedure.* Choose a desired FDR level $q \in (0, 1)$. In order to control the FDR at the level q , we apply the Benjamini-Hochberg procedure to the obtained p-values. This results in new, FDR-corrected, solution $\hat{\mathbf{u}}^{(1)}$ and $\hat{\mathbf{v}}^{(1)}$, by setting

$$\hat{u}_i^{(1)} := \begin{cases} (X^T Y \hat{\mathbf{v}}^{(0)})_i, & \text{for any rejected } H_i^{(u)}, \\ 0, & \text{otherwise.} \end{cases}$$

$$\hat{v}_j^{(1)} := \begin{cases} (Y^T X \hat{\mathbf{u}}^{(0)})_j, & \text{for any rejected } H_j^{(v)}, \\ 0, & \text{otherwise.} \end{cases}$$

For brevity of notation, in the following we denote

$$\hat{\mathbf{u}} := \hat{\mathbf{u}}^{(1)} \quad \text{and} \quad \hat{\mathbf{v}} := \hat{\mathbf{v}}^{(1)}.$$

Of course every step in the procedure would benefit from a larger size of the utilized subsample, and there is a trade-off between n_0 and n_1 to be made. However, for simplicity of exposition, in what follows we always use two subsamples of equal size, i.e., $n_0 = \lceil n/2 \rceil$.

As evidenced by the derivation of the method, the FDR correction step adapts the sparsity of the estimator to the unknown true sparsity of the solution.

V. SIMULATION STUDIES

We performed a number of simulation studies, in order to evaluate the performance of the proposed FDR-corrected sparse CCA procedure in both idealized and more realistic scenarios. The procedure, given in Section IV-B, was derived based on the assumption that X and Y have Gaussian entries. Here, we first present simulation results under such Gaussian scenarios, in order to verify that the proposed procedure indeed controls the FDR under the assumptions that its derivation relies on. Then we show simulation studies evaluating the performance of the method on non-Gaussian data, which are generated based on real single-nucleotide polymorphism (SNP) data, and closely resemble the data in the real imaging genomics application presented in Section VI.

A. Simulation study with Gaussian data

We consider scenarios where $n \gg p_X, p_Y$ (low-dimensional case), as well as where $n \ll p_X, p_Y$ (high-dimensional case). The exact data dimensions that we consider for the simulations in this section are $X \in \mathbb{R}^{500 \times 50}$ and $Y \in \mathbb{R}^{500 \times 100}$ in the low-dimensional case, and $X \in \mathbb{R}^{500 \times 1500}$ and $Y \in \mathbb{R}^{500 \times 3000}$ in the high-dimensional case. That is, $n = 500$, $p_X \in \{50, 1500\}$, and $p_Y \in \{100, 3000\}$. We denote by s_X the number of variables in X that are truly cross-correlated (i.e., have a non-zero correlation) with some variables in Y . Likewise, we denote by s_Y the number of variables in Y that are truly cross-correlated

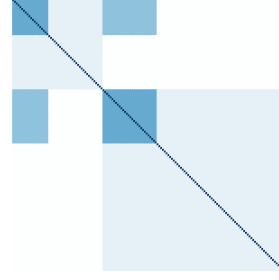


Fig. 1. An example of the covariance matrix Σ as defined by equations (12) and (13).

with some variables in X . For the simulations in this section we consider all combinations between $s_X \in \{1, 10, 20\}$ and $s_Y \in \{5, 30, 60\}$. The matrices Σ^X , Σ^Y , and Σ^{XY} are block-wise constant, and are populated with the following entries.

$$\rho_{i,j}^X = \begin{cases} 1, & \text{if } i = j, \\ 0.5, & \text{if } i \neq j, i \leq s_X, j \leq s_X, \\ 0.1, & \text{otherwise.} \end{cases}$$

$$\rho_{i,j}^Y = \begin{cases} 1, & \text{if } i = j, \\ 0.5, & \text{if } i \neq j, i \leq s_Y, j \leq s_Y, \\ 0.1, & \text{otherwise.} \end{cases} \quad (12)$$

$$\rho_{ij}^{XY} = \begin{cases} 0.4, & \text{if } i \leq s_X, j \leq s_Y, \\ 0, & \text{otherwise.} \end{cases}$$

In particular, the cross-correlation between features of X and Y is of only mediocre strength, having a magnitude of 0.4. Furthermore, the choice of parameters given in Equation (12) ensures that the covariance matrix

$$\Sigma = \begin{bmatrix} \Sigma_X & \Sigma_{XY} \\ \Sigma_{XY}^T & \Sigma_Y \end{bmatrix} \quad (13)$$

is positive definite. A visualization of one such Σ is given in Figure 1.

We perform the FDR-corrected sparse CCA procedure of Section IV-B with three choices for the target FDR level $q = 0.05, 0.1, 0.2$. For step 2 of the procedure we use the R package PMA [2] with the penalty parameters fixed at 0.9 in the low-dimensional case (the parameter has to be between 0 and 1, where a larger value corresponds to less penalization); and, in the high-dimensional case ($n < p_X, p_Y$), with the penalty parameters tuned such that $\hat{\mathbf{u}}^{(0)}$ and $\hat{\mathbf{v}}^{(0)}$ each contain approximately $\frac{n}{4}$ non-zero entries. Note that by enforcing the sparsity of $\hat{\mathbf{u}}^{(0)}$ and $\hat{\mathbf{v}}^{(0)}$ to be approximately $\frac{n}{4}$ in the high-dimensional case, we implicitly assume that $s_X, s_Y < \frac{n}{4} = 125$, which is true for the considered experiments. Had the true sparsity satisfied $s > \frac{n}{4}$, then the power of the method would decrease, because the preliminary estimates $\hat{\mathbf{u}}^{(0)}$ and $\hat{\mathbf{v}}^{(0)}$ would never contain all of the relevant features. Essentially, this amounts to having prior knowledge that the true sparsity is at most $\frac{n}{4}$ (but likely far less).

The procedure is performed 1000 times for every combination of the considered values for n , p_X , p_Y , s_X , s_Y , and q . In every considered setting, we estimate $\text{FDR}(\hat{\mathbf{u}})$ and $\text{FDR}(\hat{\mathbf{v}})$ as the mean values of the false discovery proportions obtained

from the respective 1000 simulations. We also record some other statistics from the simulations, such as the sensitivity of the proposed FDR-correction procedure.

Figure 2 shows the estimated FDR (\hat{v}) (the estimated FDR (\hat{u}) is practically identical). We observe that the estimated FDR consistently stays below the target upper bound q . Especially in the very sparse and high-dimensional scenarios the procedure seems rather conservative, having an estimated FDR that is very close to zero.

Figure 3 shows the estimated mean number of true positive discoveries that the FDR-corrected sparse CCA procedure with $q = 0.1$ results in under every scenario. We observe that the procedure tends to pick up all of the cross-correlated variables when $n \gg p_X, p_Y$. However, it is far less sensitive in the high-dimensional case $n \ll p_X, p_Y$. Additionally, in our simulations we observe that the procedure has a strong tendency to either select all of the cross-correlated features or none, rarely achieving a number in between the two extremes. This is visualized in Figure 4, which shows a histogram of the true positive proportions (TPP) obtained for all simulations with $q = 0.1$, where TPP is defined as

$$\begin{aligned} \text{TPP}(\hat{u}) &:= \frac{V_{\hat{u}}}{s_X}, \\ \text{TPP}(\hat{v}) &:= \frac{V_{\hat{v}}}{s_Y}. \end{aligned}$$

On the other hand, in each individual repetition of the experiment, the procedure generally tends to result in a false discovery proportion (FDP) far below the target upper bound on FDR. This is also shown in Figure 4, which presents a histogram of the FDP values obtained in the performed simulations with $q = 0.1$.

Summing everything up, the simulation studies of this section support the theoretical derivation of the FDR-controlling sparse CCA procedure defined in Section IV-B. As expected, the method controls the false discovery rates at the specified level q very well, when applied to Gaussian data. This adds empirical evidence to the properties implied by the mathematical derivation.

B. Simulation study with non-Gaussian data (investigating robustness to distributional assumptions)

In this section we consider more realistic simulation studies in the context of imaging genomics. The matrix X represents the SNP data, which are not normally distributed, and the matrix Y represents the contrast map data obtained from brain fMRI, which here we assume to be approximately normal. We use real SNP data, which are also used in the real data analysis of Section VI (see Section VI-A for more detail about the data), to generate X as described in the following. There are $n = 956$ subjects (rows) in the dataset. Within each gene, PCA was performed on the SNPs that belong to that gene, and only the principal components that explain at least 75% of the variance within each gene were kept as features (i.e., columns of X) for further analysis. Many of the resulting variables are clearly non-Gaussian, because many

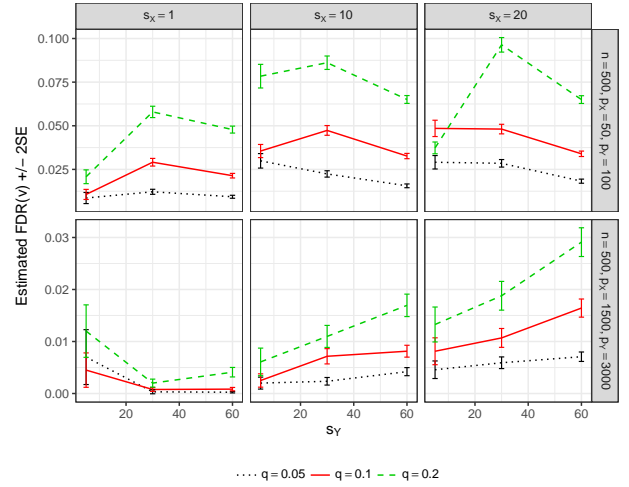


Fig. 2. FDR is estimated under multiple scenarios, which differ with respect to the number of truly cross-correlated variables in X and in Y (s_X and s_Y respectively), the sample size, and the total number of features (covering the cases $n \gg p_X, p_Y$ as well as $p_X, p_Y \gg n$). The canonical vectors are obtained via FDR-corrected sparse CCA with different choices of the target FDR level $q = 0.05, 0.1, 0.2$. The simulation is repeated 1000 times at each condition. Error bars correspond to $\pm 2SE$ (standard error).

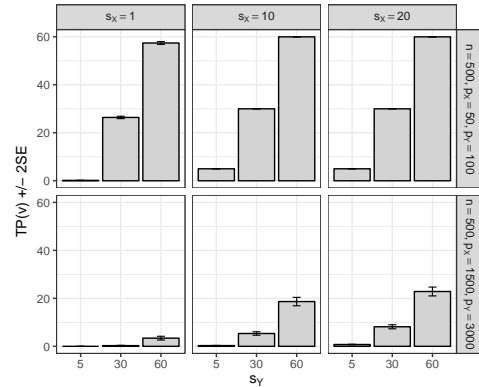


Fig. 3. Average number of entries of \mathbf{v} correctly identified as non-zero (i.e., the number of true positives, or TP) is shown under multiple conditions, which differ with respect to the number of truly cross-correlated variables in X and in Y (s_X and s_Y respectively), the sample size, and the total number of features (covering the cases $n \gg p_X, p_Y$ as well as $p_X, p_Y \gg n$). The canonical vectors are obtained via FDR-corrected sparse CCA with target FDR level $q = 0.1$, and the simulation is repeated 1000 times at each condition. Error bars correspond to $\pm 2SE$.

variables are heavily skewed, and many are clearly discrete.² Of the generated 60372 genomic features, $p_X = 10000$ variables are randomly selected to form the matrix X in each repetition of the simulation. The matrix Y is randomly sampled with independent standard normal entries, consisting of $p_Y = 10000$ columns. Finally, X and Y are standardized to have sample mean equal to zero, and sample standard deviation equal to one for each column.

We cross-correlate the data in X and Y via the following

²For example, of the resulting 60372 variables, 8356 attain 10 or fewer distinct values, and (after standardization to sample standard deviation of 1) the method of moments estimator of skewness is greater than 1 for about 10% of all variables, and great than $\frac{1}{2}$ for about 28% of all variables.

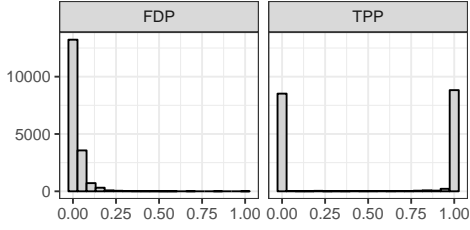


Fig. 4. The histogram on the left compares the false discovery proportions (FDP) obtained for all conditions in all performed simulations of Section V-A. The histogram on the right shows the corresponding true positive proportions (TPP). We see that the FDR-corrected sparse CCA procedure mostly results in FDP far below the target upper bound $q = 0.1$, and that it tends to either select all the relevant features or none, rarely achieving a TPP in between the two extremes.

procedure. Given, the number of cross-correlated features, $s \in \{1, 2, \dots, p\}$, where $p := p_X = p_Y$, and a parameter $\rho^{XY} \in (0, 1)$, we first generate a latent variable $\mathbf{z} \in \mathbb{R}^n$ with standard normal entries. Then, for each $i \in \{1, 2, \dots, s\}$, we replace the column \mathbf{x}_i of X with

$$\left(\sqrt{1 - \rho^{XY}}\right) \mathbf{x}_i + \left(\sqrt{\rho^{XY}}\right) \mathbf{z},$$

and likewise we replace \mathbf{y}_i with

$$\left(\sqrt{1 - \rho^{XY}}\right) \mathbf{y}_i + \left(\sqrt{\rho^{XY}}\right) \mathbf{z}.$$

Thus, after the transformation, for the cross-correlated data it holds that

$$\text{Cor}(\mathbf{x}_i, \mathbf{y}_j) = \text{Var}\left(\left(\sqrt{\rho^{XY}}\right) \mathbf{z}\right) = \rho^{XY},$$

for all $i, j \in \{1, 2, \dots, s\}$.

The considered numbers of cross-correlated variables are $s = 30, 60, 90, 120, 150, 180, 210$. For the amount of cross-correlation we consider two choices, $\rho^{XY} = 0.5$ and $\rho^{XY} = 0.9$ (we restrict the presentation to positive cross-correlations, because negative cross-correlations did not yield any noticeable changes in the simulation results). The simulation with each combination of parameters is performed 200 times.

We apply our FDR-corrected sparse CCA procedure with a target level $q = 0.1$ to this non-Gaussian dataset. In step 2 of the procedure, we tune the penalty parameters such that the preliminary estimates $\hat{\mathbf{u}}^{(0)}$ and $\hat{\mathbf{v}}^{(0)}$ each contain approximately $\frac{n}{4} = 239$ non-zero entries (see Section V-A for a brief discussion of this choice). Figure 5 shows that the estimated FDR ($\hat{\mathbf{u}}$) and FDR ($\hat{\mathbf{v}}$) levels are always far below the target upper bound. This is consistent with the application of the proposed method to high-dimensional Gaussian data, discussed in Section V-A and shown in Figure 2. Similar to the results of Section V-A on Gaussian data, shown in Figure 3, we observe that in the non-Gaussian simulations too, the procedure tends to either select all s cross-correlated features or none, rarely achieving a true positive proportion that falls between the two extremes. This is visualized in the form of a histogram in Figure 6. As one would expect, the number of instances with TPP = 0 decreases, when the magnitude of cross-correlation, ρ^{XY} , increases.

To summarize, we conclude that the proposed procedure retains its FDR-controlling properties on this non-Gaussian

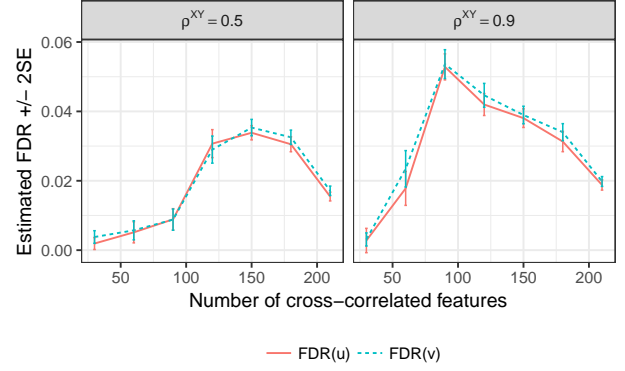


Fig. 5. Estimated FDR($\hat{\mathbf{u}}$) and FDR($\hat{\mathbf{v}}$) resulting from an application of the proposed FDR-corrected sparse CCA procedure on “hybrid” data, which consist of a matrix $X \in \mathbb{R}^{956 \times 10000}$ based on real SNP data, and a matrix $Y \in \mathbb{R}^{956 \times 10000}$ with random Gaussian entries. The parameter ρ^{XY} signifies the amount of cross-correlation between features of X and Y . The estimated FDR stays below the target upper bound $q = 0.1$ regardless of the number of truly cross-correlated features.

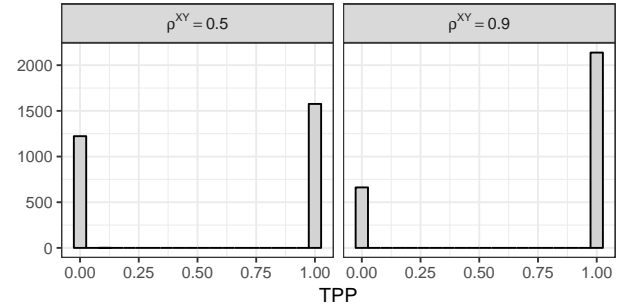


Fig. 6. Histogram of true positive proportions (TPP) observed in the simulations on non-Gaussian data of Section V-B. The FDR-corrected sparse CCA procedure tends to select either all cross-correlated features or none, rarely achieving a value in between the two extremes. The number of instances with TPP = 0 decreases, when the magnitude of cross-correlation, denoted ρ^{XY} , increases.

dataset, which is structured similarly to the real data analysed in the next section. In fact, it does not perform much differently than it performs on the Gaussian dataset. This gives us confidence on the application of the proposed procedure to real data.

VI. APPLICATION TO IMAGING GENOMICS

A. Data acquisition

The Philadelphia Neurodevelopmental Cohort [12] (PNC) is a large-scale collaborative study between the Brain Behaviour Laboratory at the University of Pennsylvania and the Children’s Hospital of Philadelphia. It contains, among other modalities, a fractal n -back fMRI task, and SNP arrays for over 900 adolescents.

The fractal n -back fMRI data were pre-processed using the software SPM12 [13]. The performed pre-processing steps included an adjustment for head movement, spatial normalization to standard MNI adult template (spatial resolution of $2\text{mm} \times 2\text{mm} \times 2\text{mm}$), and a spatio-temporal smoothing with a 3mm FWHM Gaussian kernel. Stimulus-on versus stimulus-off contrast maps were extracted for analysis. We discarded

voxels with more than 1% missing data, which resulted in a dataset consisting of 85796 voxels.

The SNP data available in the PNC were acquired using 6 different platforms. We kept only the subjects genotyped by the four most commonly used platforms (all manufactured by Illumina). The PLINK software [14] was used to pre-process the SNP data. The resulting dataset contains values for 98804 SNPs, representing the presence of two minor alleles by 2, one minor allele by 1, and the absence of a minor allele by 0 (as is the common practice).

B. Identification of cross-correlations between genomic features and brain voxels

We apply the FDR-corrected sparse CCA procedure, defined in Section IV-B, to the SNP data and the n -back fMRI contrast maps from PNC. The subset of PNC subjects for whom we have both types of data (SNP and n -back fMRI) available is of size $n = 857$. As already described in Section V-B, we apply a gene-specific PCA transformation to the SNP data. Within each gene, PCA is performed on the SNPs that belong to that gene, and within each gene only the principal components that explain at least 75% of the variance across the sample are kept as features for further analysis. This transformation results in $p_X = 60372$ genomic features, which form the matrix X . The matrix Y contains the contrast maps obtained from the n -back fMRI data. It has $p_Y = 85796$ columns, where we replace the missing values with voxel-wise averages. The columns of X and Y are standardized to have sample means equal to zero, and sample standard deviations equal to one.

Our goal is to identify the essential regions of cross-correlation between the brain voxels and the genomic features. The CCA results can help explain how genetic variation influences the brain activity fMRI data during the n -back working memory task. To that end, we apply the FDR-corrected sparse CCA procedure of Section IV-B with an upper bound of $q = 0.1$ on the false discovery rates. In step 2 of the procedure we tune the penalty parameters such that $\hat{\mathbf{u}}^{(0)}$ and $\hat{\mathbf{v}}^{(0)}$ each contain approximately $\frac{n}{4} = 214.25$ non-zero entries. The obtained FDR-corrected sparse CCA solution $\{\hat{\mathbf{u}}, \hat{\mathbf{v}}\}$ consists of 65 genomic features, which fall into 65 distinct genes, and 175 brain voxels, which fall into 6 distinct regions of interest (ROI). Figure 7 shows the brain voxels corresponding to the coefficients, which were identified as truly non-zero, as well as the genes corresponding to the genomic features identified as truly cross-correlated with the brain voxels.

A literature search confirmed that a majority of the identified genes (at least 34 out of the 65) have been previously associated with various aspects of human cognitive function. Eight of the identified genes have been previously reported in association with intelligence or cognitive performance in general (FHIT [15], CSMD1 [16], WWOX [17], SLC6A1 [18], PARK2 [19], LRP1B [20], CAMTA1 [21], THRB [22]). Seventeen genes have been previously associated with neurodevelopmental disorders, including autism spectrum disorder (RBFOX1 [23], MACROD2 [24], RORA [25], FHIT [26], GAD1 [27], AANAT [28], DAB1 [29], GRM7 [30], CNTN4 [31], PARK2 [32], NRXN3 [33]), attention deficit hyperactivity disorder (FHIT [34], GRM7 [35], CCSER1 [36], SLC6A1

[34], PARK2 [37]), and other types of neurodevelopmental disorders (SOX5 [38], CNTN4 [39], SYT14 [40], NPAS3 [41]). Furthermore, 13 genes have been associated with schizophrenia, several genes have been linked with multiple other mental disorders, and several have been found to play a role in brain development. Due to space constraints a full citation list is provided in the supporting materials. Additionally, according to GTEx (<https://gtexportal.org>), 31 out of the 65 identified genes are overexpressed in the brain.

These findings agree with our expectations. Considering that we are analysing data which result from a working memory task, the observed overlap of our results with those from previous work on other measures of cognitive performance is no surprise. Furthermore, it is reasonable to see connections with previous studies on neurodevelopmental disorders, because the PNC subjects belong to an age range (8-21) at which crucial processes of neurodevelopment are taking place. In fact, a recent study [42] observes a notable variability in the PNC cohort with respect to brain dysfunction, where additionally to a group of healthy controls consisting of 153 PNC subjects, three groups were formed as having increased (prodromal) symptoms of attention deficit disorder (107 PNC subjects), schizophrenia (103 PNC subjects), and depression (85 PNC subjects).

We group the selected voxels using the region of interest (ROI) definitions of the AAL parcellation map [43]. The identified voxels lie predominantly in the left occipital lobe. The most significant findings, as judged by the p-values from step 3 of the FDR-corrected CCA procedure of Section IV-B, correspond to the middle occipital gyri (13 selected voxels). Additional selected voxels lie in the left and right calcarine sulcus (158 voxels), left cuneus (3 voxels), and left lingual gyrus (1 voxel). Similar brain regions have been found in other fMRI studies of working memory. For example, a recent study [44], that integrates simultaneously collected EEG and fMRI data, identifies activation of the middle occipital gyrus, the cuneus, and the lingual gyrus in an investigation of the spatio-temporal activities of P3 peak during an n -back task. Another study [45], a comparative study between children and young adults, reports the functional significance of the inferior occipital lobe during an n -back task. Furthermore, as mentioned in [46], several n -back studies reported significant differences between healthy controls and attention deficit hyperactivity disorder patients in the occipital lobe, more specifically, cuneus and lingual gyrus. Additionally, the left cuneus region showed significant differences in terms of amplitude of low-frequency fluctuations of the BOLD signal during n -back task between early schizophrenic patients and healthy controls in [47].

In summary, we find previous work that supports our findings, showing genes and ROIs linked to working memory in a large adolescent study.

VII. DISCUSSION

As discussed in Section I, model selection in sparse CCA, especially as it pertains to the unknown sparsity level, is largely an unsolved problem. In this work we have proposed a notion of FDR in the context of sparse CCA as a criterion

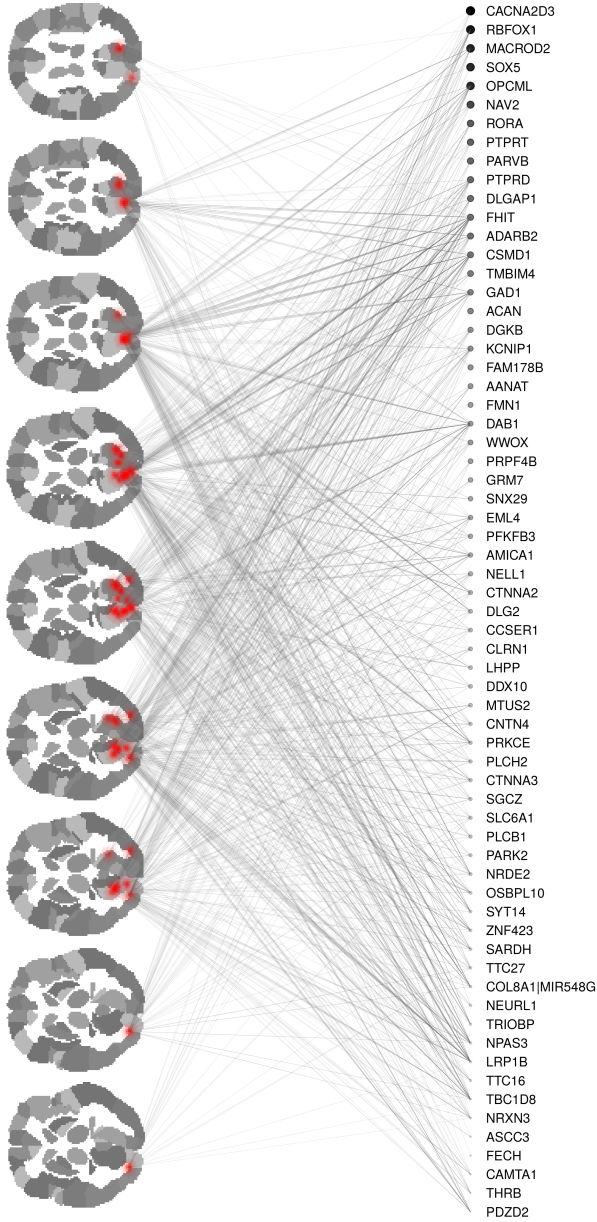


Fig. 7. Brain voxels and genes identified by the FDR-corrected sparse CCA method based on a working-memory related fMRI sequence from the PNC dataset. The selected voxels are highlighted after spatial smoothing was performed for better visibility. The color and/or size of the gene-specific and voxel-specific points correspond to the magnitude of their respective CCA coefficients. The connecting lines represent pairwise Pearson correlation coefficients between the selected voxels and genes, where line color corresponds to the magnitude of the correlation.

for the selection of an appropriate sparsity level. At the same time we have proposed an FDR-corrected sparse CCA method, which is adaptive to the unknown true sparsity of the canonical vectors. With theoretical arguments and a series of simulation studies we have shown that the proposed method controls the FDR of sparse CCA estimators at a user-specified level.

Interestingly, even though our method was analytically de-

rived under Gaussian assumptions (and certain assumption of stochastic independence), in the considered non-Gaussian simulations (which also violated the independence assumptions) it still achieved FDR control. Thus it would be interesting to extend the theoretical argumentation for FDR control of the proposed method beyond the Gaussian scenarios. It would also be interesting to investigate how the sparsity constraints on the preliminary estimates $\hat{\mathbf{u}}^{(0)}$ and $\hat{\mathbf{v}}^{(0)}$ can be made liberal enough, such that additional (preferably all) cross-correlated features of X and Y are identified. Especially in the high-dimensional case a trade-off arises, because when $\hat{\mathbf{u}}^{(0)}$ and $\hat{\mathbf{v}}^{(0)}$ are too dense, it not only becomes harder to estimate Σ well, but the FDR-correction step can significantly lose power as well. Furthermore, especially in high-dimensional scenarios, the proposed method tends to be too conservative, having an FDR far below the nominal level. An adjustment that would result in an FDR closer to the nominal level is very desirable, because it would increase the detection power. These are the important open questions that we leave for future research.

APPENDIX A ASYMPTOTIC NORMALITY PROOF

In this Section we present the proof of Theorem 1. We need the following Lemma.

Lemma 1. Assume that $A \in \mathbb{R}^{p \times p}$ and $B \in \mathbb{R}^{p \times p}$ are symmetric matrices. Let $S \in \mathbb{R}^{p \times p}$ be a random matrix that follows a Wishart distribution with parameters $\Sigma \in \mathbb{R}^{p \times p}$, p and n . Then it holds that

$$\text{Cov}(\text{tr}(AS), \text{tr}(BS)) = \text{tr}(2nA\Sigma B\Sigma).$$

Proof. Because A and B are symmetric, we have that

$$\begin{aligned} \text{Cov}(\text{tr}(AS), \text{tr}(BS)) &= \text{Cov}\left(\sum_{i,j=1,\dots,p} a_{ij}s_{ij}, \sum_{k,l=1,\dots,p} b_{kl}s_{kl}\right) \\ &= \sum_{i,j=1,\dots,p} a_{ij} \sum_{k,l=1,\dots,p} b_{kl} \text{Cov}(s_{ij}, s_{kl}) \\ &= \sum_{i,j=1,\dots,p} a_{ij} [\text{mat}(\text{Cov}(\text{vec}(S)) \cdot \text{vec}(B))]_{ij} \\ &= \text{tr}(A \cdot \text{mat}(\text{Cov}(\text{vec}(S))\text{vec}(B))), \end{aligned}$$

where $\text{vec}(\cdot)$ denotes vectorization, and $\text{mat}(\cdot)$ denotes matricization (i.e., the inverse of vectorization).

Now, Proposition 8.3 in [48] together with Kronecker product properties implies that

$$\begin{aligned} \text{Cov}(\text{tr}(AS), \text{tr}(BS)) &= \text{tr}(A \cdot \text{mat}((2n\Sigma \otimes \Sigma)\text{vec}(B))) \\ &= 2n\text{tr}(A\Sigma B\Sigma). \end{aligned}$$

□

A. Proof of Theorem 1

Proof. Because the random vectors $(\mathbf{x}_1^T, \mathbf{y}_1^T)^T$, $(\mathbf{x}_2^T, \mathbf{y}_2^T)^T$, \dots , $(\mathbf{x}_n^T, \mathbf{y}_n^T)^T$ are independent and identically distributed, and since

$$\frac{1}{n} X^T Y \mathbf{v} = \frac{1}{n} \sum_{k=1}^n \mathbf{x}_k \mathbf{y}_k^T \mathbf{v},$$

the multidimensional version of the Central Limit Theorem immediately gives

$$\sqrt{n} \left(\frac{1}{n} X^T Y \mathbf{v} - \boldsymbol{\mu} \right) \xrightarrow{\mathcal{D}} \mathcal{N}(0, \Omega),$$

where

$$\boldsymbol{\mu} = \mathbb{E}(\mathbf{x}_k \mathbf{y}_k^T \mathbf{v}), \quad (14)$$

$$\Omega = \text{Cov}(\mathbf{x}_k \mathbf{y}_k^T \mathbf{v}), \quad (15)$$

for all $k \in \{1, 2, \dots, n\}$.

Now, it is left to prove that the entries of $\boldsymbol{\mu}$ and Ω have the form specified in equations (10) and (11).

Equation (10) follows directly from the linearity of expectation and the fact that all entries of X and Y are Gaussian with mean zero.

For notational convenience, denote $A := \begin{bmatrix} X & Y \end{bmatrix}$ and $\mathbf{w} := \frac{1}{n} X^T Y \mathbf{v}$. In order to prove (11), we first observe that $A^T A \sim \tilde{W}(\Sigma, p_X + p_Y, n)$, which denotes a Wishart distribution with parameters Σ , $(p_X + p_Y)$ and n , where Σ is defined by equation (1). Then we also observe that

$$\text{tr} \left(\frac{1}{2n} \begin{bmatrix} 0 & \mathbf{e}_i \mathbf{v}^T \\ \mathbf{v} \mathbf{e}_i^T & 0 \end{bmatrix} \cdot A^T A \right) = w_i,$$

where $\mathbf{e}_i \in \mathbb{R}^P$ denotes the i th standard basis vector in \mathbb{R}^{p_X} .

Thus, using Lemma 1, we conclude that

$$\begin{aligned} \text{Cov}(w_i, w_j) &= \\ &= 2n \cdot \text{tr} \left(\frac{1}{2n} \begin{bmatrix} 0 & \mathbf{e}_i \mathbf{v}^T \\ \mathbf{v} \mathbf{e}_i^T & 0 \end{bmatrix} \cdot \Sigma \cdot \frac{1}{2n} \begin{bmatrix} 0 & \mathbf{e}_j \mathbf{v}^T \\ \mathbf{v} \mathbf{e}_j^T & 0 \end{bmatrix} \cdot \Sigma \right) \\ &= \frac{1}{2n} \text{tr} \left(\begin{bmatrix} \mathbf{e}_i \mathbf{v}^T \Sigma_{XY}^T & \mathbf{e}_i \mathbf{v}^T \Sigma_Y \\ \mathbf{v} \mathbf{e}_i^T \Sigma_X & \mathbf{v} \mathbf{e}_i^T \Sigma_{XY} \end{bmatrix} \cdot \begin{bmatrix} \mathbf{e}_j \mathbf{v}^T \Sigma_{XY}^T & \mathbf{e}_j \mathbf{v}^T \Sigma_Y \\ \mathbf{v} \mathbf{e}_j^T \Sigma_X & \mathbf{v} \mathbf{e}_j^T \Sigma_{XY} \end{bmatrix} \right) \\ &= \frac{1}{2n} \left\{ \text{tr}(\mathbf{e}_i \mathbf{v}^T \Sigma_{XY}^T \mathbf{e}_j \mathbf{v}^T \Sigma_{XY}^T) + \text{tr}(\mathbf{e}_i \mathbf{v}^T \Sigma_Y \mathbf{v} \mathbf{e}_j^T \Sigma_X) \right. \\ &\quad \left. + \text{tr}(\mathbf{v} \mathbf{e}_i^T \Sigma_X \mathbf{e}_j \mathbf{v}^T \Sigma_Y) + \text{tr}(\mathbf{v} \mathbf{e}_i^T \Sigma_{XY} \mathbf{v} \mathbf{e}_j^T \Sigma_{XY}) \right\} \\ &= \frac{1}{2n} \left\{ 2\text{tr}(\mathbf{e}_i \mathbf{v}^T \Sigma_{XY}^T \mathbf{e}_j \mathbf{v}^T \Sigma_{XY}^T) + 2\text{tr}(\mathbf{v}^T \Sigma_Y \mathbf{v} \mathbf{e}_j^T \Sigma_X \mathbf{e}_i) \right\} \\ &= \frac{1}{n} \left\{ \left(\sum_{k=1}^{p_Y} v_k \rho_{j,k}^{XY} \right) \left(\sum_{k=1}^{p_Y} v_k \rho_{i,k}^{XY} \right) + \mathbf{v}^T \Sigma_Y \mathbf{v} \rho_{j,i}^X \right\} \quad (16) \end{aligned}$$

Moreover, we have that

$$\begin{aligned} \text{Cov}(\mathbf{w}) &= \text{Cov} \left(\frac{1}{n} \sum_{k=1}^n \mathbf{x}_k \mathbf{y}_k^T \mathbf{v} \right) \\ &= \frac{1}{n^2} \sum_{k=1}^n \text{Cov}(\mathbf{x}_k \mathbf{y}_k^T \mathbf{v}) = \frac{1}{n} \Omega, \quad (17) \end{aligned}$$

where we used equation (15) and the fact that the random vectors $(\mathbf{x}_1^T, \mathbf{y}_1^T)^T$, $(\mathbf{x}_2^T, \mathbf{y}_2^T)^T$, \dots , $(\mathbf{x}_n^T, \mathbf{y}_n^T)^T$ are independent and identically distributed.

Finally, equation (16) combined with equation (17) yield equation (11). \square

ACKNOWLEDGMENT

The work was partially supported by NIH (R01 GM109068, R01 MH104680, R01 MH107354, P20 GM103472, R01 REB020407, R01 EB006841) and NSF (#1539067).

REFERENCES

- [1] H. Hotelling, "Relations between two sets of variates," *Biometrika*, 1936.
- [2] D. M. Witten, R. Tibshirani, and T. Hastie, "A penalized matrix decomposition, with applications to sparse principal components and canonical correlation analysis," *Biostatistics*, vol. 10, no. 3, pp. 515–534, Jul. 2009.
- [3] D. M. Witten and R. J. Tibshirani, "Extensions of sparse canonical correlation analysis with applications to genomic data," *Statistical applications in genetics and molecular biology*, vol. 8, 9 Jun. 2009.
- [4] E. Parkhomenko, D. Tritchler, and J. Beyene, "Sparse canonical correlation analysis with application to genomic data integration," *Statistical applications in genetics and molecular biology*, vol. 8, 6 Jan. 2009.
- [5] K.-A. Lê Cao, P. G. P. Martin, C. Robert-Granié, and P. Besse, "Sparse canonical methods for biological data integration: application to a cross-platform study," *BMC bioinformatics*, vol. 10, p. 34, 26 Jan. 2009.
- [6] S. Waaijenborg, P. C. Verselewe de Witt Hamer, and A. H. Zwinderman, "Quantifying the association between gene expressions and DNA-markers by penalized canonical correlation analysis," *Statistical applications in genetics and molecular biology*, vol. 7, no. 1, 23 Jan. 2008.
- [7] D. Lin, V. D. Calhoun, and Y.-P. Wang, "Correspondence between fMRI and SNP data by group sparse canonical correlation analysis," *Medical image analysis*, vol. 18, no. 6, pp. 891–902, Aug. 2014.
- [8] L. Du, H. Huang, J. Yan, S. Kim, S. L. Risacher, M. Inlow, J. H. Moore, A. J. Saykin, L. Shen, and Alzheimers Disease Neuroimaging Initiative, "Structured sparse canonical correlation analysis for brain imaging genetics: an improved GraphNet method," *Bioinformatics*, vol. 32, no. 10, pp. 1544–1551, 15 May 2016.
- [9] I. Wilms and C. Croux, "Sparse canonical correlation analysis from a predictive point of view," *Biometrical journal. Biometrische Zeitschrift*, vol. 57, no. 5, pp. 834–851, Sep. 2015.
- [10] Y. Benjamini and Y. Hochberg, "Controlling the False Discovery Rate: A Practical and Powerful Approach to Multiple Testing," *Journal of the Royal Statistical Society. Series B, Statistical methodology*, vol. 57, no. 1, pp. 289–300, 1995.
- [11] R. A. Johnson and D. W. Wichern, *Applied multivariate statistical analysis*, 6th ed. Prentice hall Upper Saddle River, NJ, 2007.
- [12] T. D. Satterthwaite, M. A. Elliott, K. Ruparel, J. Loughhead, K. Prabhakaran, M. E. Calkins, R. Hopson, C. Jackson, J. Keefe, M. Riley *et al.*, "Neuroimaging of the Philadelphia neurodevelopmental cohort," *NeuroImage*, vol. 86, pp. 544–553, 1 Feb. 2014.
- [13] J. Ashburner, G. Barnes, C.-C. Chen, J. Daunizeau, G. Flandin, K. Friston, S. Kiebel, J. Kilner, V. Litvak, R. Moran *et al.*, "SPM12 Manual The FIL Methods Group (and honorary members)," 2014.
- [14] S. Purcell, B. Neale, K. Todd-Brown, L. Thomas, M. A. R. Ferreira, D. Bender, J. Maller, P. Sklar, P. I. W. de Bakker, M. J. Daly, and P. C. Sham, "PLINK: a tool set for whole-genome association and population-based linkage analyses," *American journal of human genetics*, vol. 81, no. 3, pp. 559–575, Sep. 2007.
- [15] O. S. P. Davis, L. M. Butcher, S. J. Docherty, E. L. Meaburn, C. J. C. Curtis, M. A. Simpson, L. C. Schalkwyk, and R. Plomin, "A three-stage genome-wide association study of general cognitive ability: hunting the small effects," *Behavior genetics*, vol. 40, no. 6, pp. 759–767, Nov. 2010.
- [16] E. Koiliari, P. Roussos, E. Pasparakis, T. Lencz, A. Malhotra, L. J. Siever, S. G. Giakoumaki, and P. Bitsios, "The CSMD1 genome-wide associated schizophrenia risk variant rs10503253 affects general cognitive ability and executive function in healthy males," *Schizophrenia research*, vol. 154, no. 1-3, pp. 42–47, Apr. 2014.
- [17] J. L. McClay, D. E. Adkins, K. Aberg, J. Bukszár, A. N. Khachane, R. S. E. Keefe, D. O. Perkins, J. P. McEvoy, T. S. Stroup, R. E. Vann *et al.*, "Genome-wide pharmacogenomic study of neurocognition as an indicator of antipsychotic treatment response in schizophrenia," *Neuropsychopharmacology: official publication of the American College of Neuropsychopharmacology*, vol. 36, no. 3, pp. 616–626, Feb. 2011.
- [18] J.-H. Hu, Y.-H. Ma, J. Jiang, N. Yang, S.-H. Duan, Z.-H. Jiang, Z.-T. Mei, J. Fei, and L.-H. Guo, "Cognitive impairment in mice over-expressing gamma-aminobutyric acid transporter 1 (GAT1)," *Neuroreport*, vol. 15, no. 1, pp. 9–12, 19 Jan. 2004.
- [19] B. R. Benbunan, A. D. Korczyn, and N. Giladi, "Parkin mutation associated parkinsonism and cognitive decline, comparison to early onset Parkinson's disease," *Journal of neural transmission*, vol. 111, no. 1, pp. 47–57, Jan. 2004.
- [20] S. E. Poduslo, R. Huang, and A. Spiro, 3rd, "A genome screen of successful aging without cognitive decline identifies LRP1B by haplotype analysis," *American journal of medical genetics. Part B, Neuropsychiatric genetics: the official publication of the International*

- Society of Psychiatric Genetics*, vol. 153B, no. 1, pp. 114–119, 5 Jan. 2010.
- [21] M. J. Huentelman, A. Papassotiropoulos, D. W. Craig, F. J. Hoerndli, J. V. Pearson, K.-D. Huynh, J. Corneveaux, J. Hänggi, C. R. A. Mondadori, A. Buchmann *et al.*, “Calmodulin-binding transcription activator 1 (CAMTA1) alleles predispose human episodic memory performance,” *Human molecular genetics*, vol. 16, no. 12, pp. 1469–1477, 15 Jun. 2007.
- [22] R. E. Weiss, M. A. Stein, S. C. Duck, B. Chyna, W. Phillips, T. O’Brien, L. Gutermuth, and S. Refetoff, “Low intelligence but not attention deficit hyperactivity disorder is associated with resistance to thyroid hormone caused by mutation R316H in the thyroid hormone receptor beta gene,” *The Journal of clinical endocrinology and metabolism*, vol. 78, no. 6, pp. 1525–1528, Jun. 1994.
- [23] B. R. Bill, J. K. Lowe, C. T. Dybuncio, and B. L. Fogel, “Orchestration of neurodevelopmental programs by RBFOX1: implications for autism spectrum disorder,” *International review of neurobiology*, vol. 113, pp. 251–267, 2013.
- [24] R. Anney, L. Klei, D. Pinto, R. Regan, J. Conroy, T. R. Magalhaes, C. Correia, B. S. Abrahams, N. Sykes, A. T. Pagnamenta *et al.*, “A genome-wide scan for common alleles affecting risk for autism,” *Human molecular genetics*, vol. 19, no. 20, pp. 4072–4082, 15 Oct. 2010.
- [25] T. Sarachana, M. Xu, R.-C. Wu, and V. W. Hu, “Sex hormones in autism: androgens and estrogens differentially and reciprocally regulate RORA, a novel candidate gene for autism,” *PLoS one*, vol. 6, no. 2, Feb. 2011.
- [26] D. Salyakina, D. Q. Ma, J. M. Jaworski, I. Konidari, P. L. Whitehead, R. Henson, D. Martinez, J. L. Robinson, S. Sacharow, H. H. Wright *et al.*, “Variants in several genomic regions associated with asperger disorder,” *Autism research: official journal of the International Society for Autism Research*, vol. 3, no. 6, pp. 303–310, Dec. 2010.
- [27] J. Yip, J.-J. Soghomonian, and G. J. Blatt, “Increased GAD67 mRNA expression in cerebellar interneurons in autism: implications for Purkinje cell dysfunction,” *Journal of neuroscience research*, vol. 86, no. 3, pp. 525–530, 15 Feb. 2008.
- [28] B. M. Anderson, N. C. Schnetz-Boutaud, J. Bartlett, A. M. Wotawa, H. H. Wright, R. K. Abramson, M. L. Cuccaro, J. R. Gilbert, M. A. Pericak-Vance, and J. L. Haines, “Examination of association of genes in the serotonin system to autism,” *Neurogenetics*, vol. 10, no. 3, pp. 209–216, Jul. 2009.
- [29] J. Li, J. Liu, L. Zhao, Y. Ma, M. Jia, T. Lu, Y. Ruan, Q. Li, W. Yue, D. Zhang, and L. Wang, “Association study between genes in Reelin signaling pathway and autism identifies DAB1 as a susceptibility gene in a Chinese Han population,” *Progress in neuro-psychopharmacology & biological psychiatry*, vol. 44, pp. 226–232, 1 Jul. 2013.
- [30] Y. Yang and C. Pan, “Role of metabotropic glutamate receptor 7 in autism spectrum disorders: a pilot study,” *Life sciences*, vol. 92, no. 2, pp. 149–153, 7 Feb. 2013.
- [31] J. Roohi, C. Montagna, D. H. Tegay, L. E. Palmer, C. DeVincent, J. C. Pomeroy, S. L. Christian, N. Nowak, and E. Hatchwell, “Disruption of contactin 4 in three subjects with autism spectrum disorder,” *Journal of medical genetics*, vol. 46, no. 3, pp. 176–182, Mar. 2009.
- [32] C.-L. Yin, H.-I. Chen, L.-H. Li, Y.-L. Chien, H.-M. Liao, M. C. Chou, W.-J. Chou, W.-C. Tsai, Y.-N. Chiu, Y.-Y. Wu *et al.*, “Genome-wide analysis of copy number variations identifies PARK2 as a candidate gene for autism spectrum disorder,” *Molecular autism*, vol. 7, p. 23, 1 Apr. 2016.
- [33] A. K. Vaags, A. C. Lionel, D. Sato, M. Goodenberger, Q. P. Stein, S. Curran, C. Ogilvie, J. W. Ahn, I. Drmic, L. Senman *et al.*, “Rare deletions at the neurexin 3 locus in autism spectrum disorder,” *American journal of human genetics*, vol. 90, no. 1, pp. 133–141, 13 Jan. 2012.
- [34] J. Lasky-Su, B. M. Neale, B. Franke, R. J. L. Anney, K. Zhou, J. B. Maller, A. A. Vasquez, W. Chen, P. Asherson, J. Buitelaar *et al.*, “Genome-wide association scan of quantitative traits for attention deficit hyperactivity disorder identifies novel associations and confirms candidate gene associations,” *American journal of medical genetics. Part B, Neuropsychiatric genetics: the official publication of the International Society of Psychiatric Genetics*, vol. 147B, no. 8, pp. 1345–1354, 5 Dec. 2008.
- [35] S. Park, S.-W. Jung, B.-N. Kim, S.-C. Cho, M.-S. Shin, J.-W. Kim, H. J. Yoo, D.-Y. Cho, U.-S. Chung, J.-W. Son, and H.-W. Kim, “Association between the GRM7 rs3792452 polymorphism and attention deficit hyperactivity disorder in a Korean sample,” *Behavioral and brain functions: BBF*, vol. 9, p. 1, 7 Jan. 2013.
- [36] F. Lantieri, J. T. Glessner, H. Hakonarson, J. Elia, and M. Devoto, “Analysis of GWAS top hits in ADHD suggests association to two polymorphisms located in genes expressed in the cerebellum,” *American journal of medical genetics. Part B, Neuropsychiatric genetics: the official publication of the International Society of Psychiatric Genetics*, vol. 153B, no. 6, pp. 1127–1133, Sep. 2010.
- [37] I. Jarick, A.-L. Volckmar, C. Pütter, S. Pechlivanis, T. T. Nguyen, M. R. Dauvermann, S. Beck, Ö. Albayrak, S. Scherag, S. Gilsbach *et al.*, “Genome-wide analysis of rare copy number variations reveals PARK2 as a candidate gene for attention-deficit/hyperactivity disorder,” *Molecular psychiatry*, vol. 19, no. 1, pp. 115–121, Jan. 2014.
- [38] A. Nesbitt, E. J. Bhoj, K. McDonald Gibson, Z. Yu, E. Denenberg, M. Sarmady, T. Tischler, K. Cao, H. Dubbs, E. H. Zackai, and A. Santani, “Exome sequencing expands the mechanism of SOX5-associated intellectual disability: A case presentation with review of sox-related disorders,” *American journal of medical genetics. Part A*, vol. 167A, no. 11, pp. 2548–2554, Nov. 2015.
- [39] T. Fernandez, T. Morgan, N. Davis, A. Klin, A. Morris, A. Farhi, R. P. Lifton, and M. W. State, “Disruption of contactin 4 (CNTN4) results in developmental delay and other features of 3p deletion syndrome,” *American journal of human genetics*, vol. 74, no. 6, pp. 1286–1293, Jun. 2004.
- [40] F. Quintero-Rivera, A. Chan, D. J. Donovan, J. F. Gusella, and A. H. Ligon, “Disruption of a synaptotagmin (SYT14) associated with neurodevelopmental abnormalities,” *American journal of medical genetics. Part A*, vol. 143A, no. 6, pp. 558–563, 15 Mar. 2007.
- [41] B. S. Pickard, M. P. Malloy, D. J. Porteous, D. H. R. Blackwood, and W. J. Muir, “Disruption of a brain transcription factor, NPAS3, is associated with schizophrenia and learning disability,” *American journal of medical genetics. Part B, Neuropsychiatric genetics: the official publication of the International Society of Psychiatric Genetics*, vol. 136B, no. 1, pp. 26–32, 5 Jul. 2005.
- [42] T. Kaufmann, D. Alnæs, N. T. Doan, C. L. Brandt, O. A. Andreassen, and L. T. Westlye, “Delayed stabilization and individualization in connectome development are related to psychiatric disorders,” *Nature neuroscience*, vol. 20, no. 4, pp. 513–515, Apr. 2017.
- [43] N. Tzourio-Mazoyer, B. Landeau, D. Papathanassiou, F. Crivello, O. Etard, N. Delcroix, B. Mazoyer, and M. Joliot, “Automated anatomical labeling of activations in SPM using a macroscopic anatomical parcellation of the MNI MRI single-subject brain,” *NeuroImage*, vol. 15, no. 1, pp. 273–289, Jan. 2002.
- [44] Q. Zhang, X. Yang, L. Yao, and X. Zhao, “Working memory load-dependent spatio-temporal activity of single-trial P3 response detected with an adaptive wavelet denoiser,” *Neuroscience*, vol. 346, pp. 64–73, 27 Mar. 2017.
- [45] K. T. Ciesielski, P. G. Lesnik, R. L. Savoy, E. P. Grant, and S. P. Ahlfors, “Developmental neural networks in children performing a categorical n-back task,” *NeuroImage*, vol. 33, no. 3, pp. 980–990, 2006.
- [46] H. McCarthy, N. Skokauskas, and T. Frodl, “Identifying a consistent pattern of neural function in attention deficit hyperactivity disorder: a meta-analysis,” *Psychological medicine*, vol. 44, no. 04, pp. 869–880, 2014.
- [47] Y. Zhou, Z. Wang, X.-N. Zuo, H. Zhang, Y. Wang, T. Jiang, and Z. Liu, “Hyper-coupling between working memory task-evoked activations and amplitude of spontaneous fluctuations in first-episode schizophrenia,” *Schizophrenia Research*, vol. 159, no. 1, pp. 80–89, 2014.
- [48] M. L. Eaton, *Multivariate statistics: a vector space approach*, ser. Lecture notes-monograph series ; v. 53. Beachwood, Ohio: Institute of Mathematical Statistics, 2007.